

Effect of solvents on the microstructure of CaWO_4 prepared by a solvothermal synthesis

Sulawan Kaowphong^{a,*}, Titipun Thongtem^b and Somchai Thongtem^c

^aDepartment of Chemistry, Faculty of Science, Naresuan University, Phitsanulok 65000, Thailand

^bDepartment of Chemistry, Faculty of Science, Chiang Mai University, Chiang Mai 50200, Thailand

^cDepartment of Physics and Materials Science, Faculty of Science, Chiang Mai University, Chiang Mai 50200, Thailand

Different sizes of nanostructured CaWO_4 have been prepared by a simple solvothermal synthesis at a low temperature of 160 °C for 6 h through the reaction between $\text{Ca}(\text{NO}_3)_2 \cdot 4\text{H}_2\text{O}$ and $\text{Na}_2\text{WO}_4 \cdot 2\text{H}_2\text{O}$ using various solvents as the reaction medium. The products, characterized by X-ray diffraction (XRD), were specified as pure CaWO_4 with the scheelite structure. Scanning electron microscope (SEM) and transmission electron microscope (TEM) analysis showed that the particle sizes are mainly related to the physical and chemical properties of the solvents used in the solvothermal synthesis. Photoluminescence properties were also investigated.

Key words: Nanocrystalline materials, Solvothermal synthesis, CaWO_4 .

Introduction

CaWO_4 compound is an important inorganic material that has been a subject of numerous investigations on its luminescent properties. It is attractive for application in lasers, and fluorescent lamps [1-4]. It is well known that the physical properties of nanomaterials are strongly related to their crystallite size and their morphology. Hence, controlling the size and morphology of nanostructures is still a major challenge. Thus far, several methods have been developed for the preparation of CaWO_4 phosphors. In solid state reactions, a high reaction temperature and a long heating time are required to obtain a pure phase. Therefore, producing agglomerated particles of irregular shape by solid state reactions is unavoidable. Furthermore, inhomogeneous compounds of metal tungstates might be formed easily because WO_3 has a tendency to vaporize at high temperatures [5-7]. Thus far, a number of attempts have been made to develop the preparation of CaWO_4 by applying soft solution methods such as a polymerized complex method [7], spray pyrolysis [8], and a metathetic reaction [9]. In this study, nanoparticles have been prepared by solvothermal synthesis using water, glycerol-water, and propylene glycol-water as the solvents. The microstructures and photoluminescence properties of the synthesized powders have been characterized and the relationship with the solvent has been investigated in detail.

Experimental procedure

In a typical synthesis, 0.003 mole $\text{Ca}(\text{NO}_3)_2 \cdot 4\text{H}_2\text{O}$ and $\text{Na}_2\text{WO}_4 \cdot 2\text{H}_2\text{O}$ was dissolved in 30 ml pure water or mixed solvents of glycerol-water (or propylene glycol-water) with the volume ratio 25/5. Then the resulting solution was loaded into a Teflon-lined stainless-steel autoclave. The autoclave was then sealed and maintained at 160 °C for 6 h for the reaction. After the system was cooled down to room temperature, the white powders in the autoclave were filtered and washed with distilled water and ethanol several times, and finally dried at 80 °C for 12 h.

The crystallinity and phase purity of the prepared samples were analyzed by an X-ray diffractometer with $\text{CuK}\alpha$ radiation (wavelength: 0.15406 nm) operating at 20 kV-15 mA in the 2θ range of 10°-60°. The morphology and particle sizes of samples were determined by a field emission-scanning electron microscope (FE-SEM, JSM-6335F) operated at 15 kV accelerating voltage and a transmission electron microscope (TEM, JEOL JEM-2010) operating at 20 kV. Fourier transform infrared spectra (FT-IR, 510 Nicolet) were acquired in the range of 400-4000 cm^{-1} . The emission spectra was measured by Perkin Elmer Luminescence spectrometer LS50B.

Results and Discussion

Fig. 1 gives the representative XRD patterns of all samples. All the diffraction peaks could be indexed to the tetragonal cell of CaWO_4 , which are consistent with reported values [10] (JCPDS file no. 77-2234). No impurity phases were detected. The sharp peaks indicated good

*Corresponding author:
Tel : +66 55 963434
Fax: +66 55 963113
E-mail: sulawank@nu.ac.th

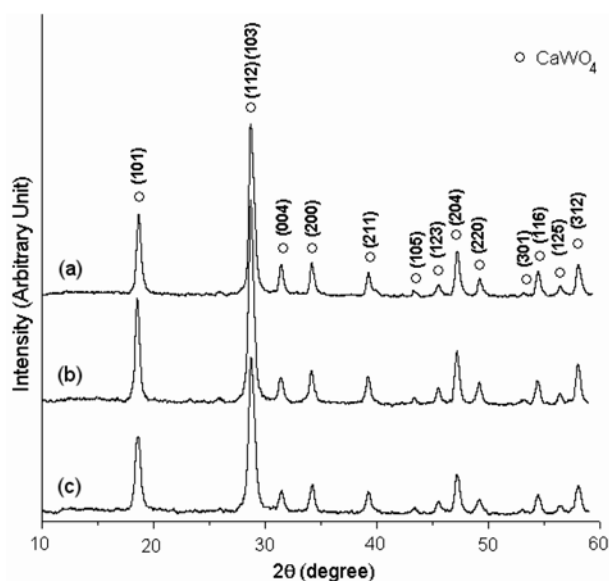


Fig. 1. XRD patterns of the CaWO_4 powders prepared in different solvents: (a) pure water, (b) glycerol-water and (c) propylene glycol-water.

crystallization of the CaWO_4 . For the CaWO_4 structure, Ca^{2+} and $[\text{WO}_4]^{2-}$ are loosely bound together and arranged as a cubic close-packed array. W ions are within tetrahedral O-ion cages and are isolated from each other, while Ca ions are surrounded by eight oxygen ions [8]. The FT-IR spectra of the CaWO_4 powders obtained in different solvents (Fig. 2(c)–(e)) revealed the presence of O–H stretching and O–H bending of residual water at $3,070\text{--}3,690\text{ cm}^{-1}$ and $1,620\text{ cm}^{-1}$ [11], respectively. The strong peak at $705\text{--}875\text{ cm}^{-1}$ is associated with the stretching vibration of the W–O bond in $[\text{WO}_4]^{2-}$ tetrahedra [12, 13], which is in accord with the detection of tungstates analyzed by XRD. Another weak W–O stretching band was detected at $409\text{--}443\text{ cm}^{-1}$ [13, 14] as well. For comparison reasons, the IR spectra of pure glycerol and propylene glycol (Fig. 2(a)–(b)) were also measured, showing absorption bands in the region $2875\text{--}2975\text{ cm}^{-1}$ characteristic of the C–H stretching vibration of hydrocarbons, the bands at $1450\text{--}1500\text{ cm}^{-1}$ attributed to the bending vibration of the C–H in the methylene group [14], and the strong band at 1044 cm^{-1} corresponding to the stretching vibration of the C–O group in the polyol molecule [15]. There are no bands specific to pure propylene glycol or glycerol in the FT-IR spectra of the CaWO_4 powders, clearly indicating that the final products have no organic impurities.

Fig. 3 shows SEM micrographs of CaWO_4 powders prepared in different solvents. The powders prepared in pure water compose of rather round nano-sized particles in irregular micro-sized clusters as shown in Fig. 3(a). The nano-sized particles formed and subsequently in clusters together in small groups. Fig. 3(b) and (c) show the SEM micrographs of the powders prepared in mixed solvents of glycerol-water and propylene glycol-water. These powders are nano-sized particles. The particle sizes

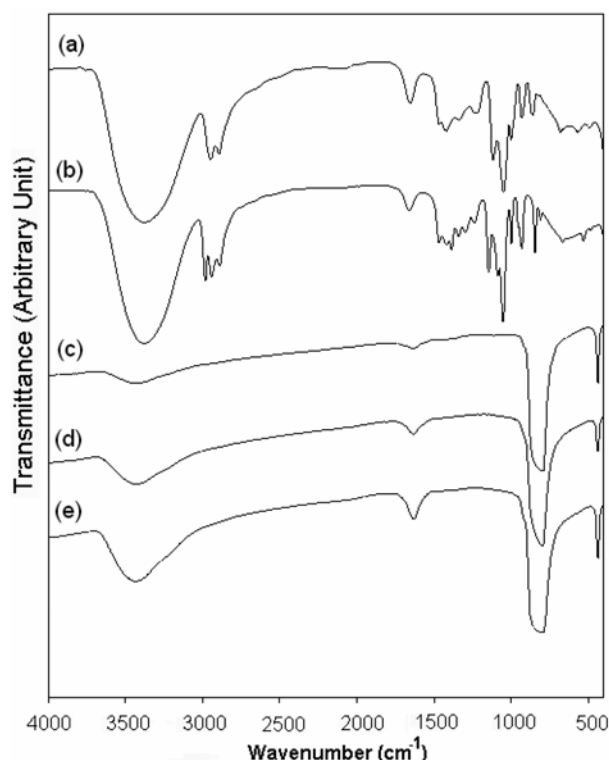


Fig. 2. FT-IR spectra of pure solvents (a) propylene glycol, (b) glycerol and those of the CaWO_4 powders prepared in different solvents (c) pure water, (d) glycerol-water and (e) propylene glycol-water.

and particle size distributions of the CaWO_4 powders were also investigated by TEM images as shown in Fig. 4 and particle size distributions shown in Fig. 5. The average sizes are 44.2 ± 13.9 , 23.3 ± 6.7 , $14.3 \pm 3.7\text{ nm}$ for the powders prepared in pure water, glycerol-water and propylene glycol-water, respectively. The main reasons for these phenomena can be expressed by considering some physical properties of different solvents used in the present research [16] as shown in Table 1. It is obvious that each solvent possessed a different boiling point, dielectric constant and thermal conductivity. For the present research, the resulting powders treated in water prefer to form with a large particle size and as high quality crystals because the higher dielectric constant and thermal conductivity correspond to the higher solubility of the inorganic solute and high diffusion rate of ions in the solution. On the other hand, in the case of using glycol solvents, because of the low diffusion rate of ions in the solvent, crystalline growth was suppressed, and led to the formation of fine nanoparticles. The dielectric constant of the solvent has an important influence on the growth rate of CaWO_4 powders during solvothermal synthesis since small particles will be more stable in a solvent with a low dielectric constant than in a solvent with a high dielectric constant. The possibility of a complex between the ions and the organic solvent will also hinder the growth of CaWO_4 particles during solvothermal synthesis [17–19]. Therefore, we believe that the properties of the solvent lead to a change of the crystallite

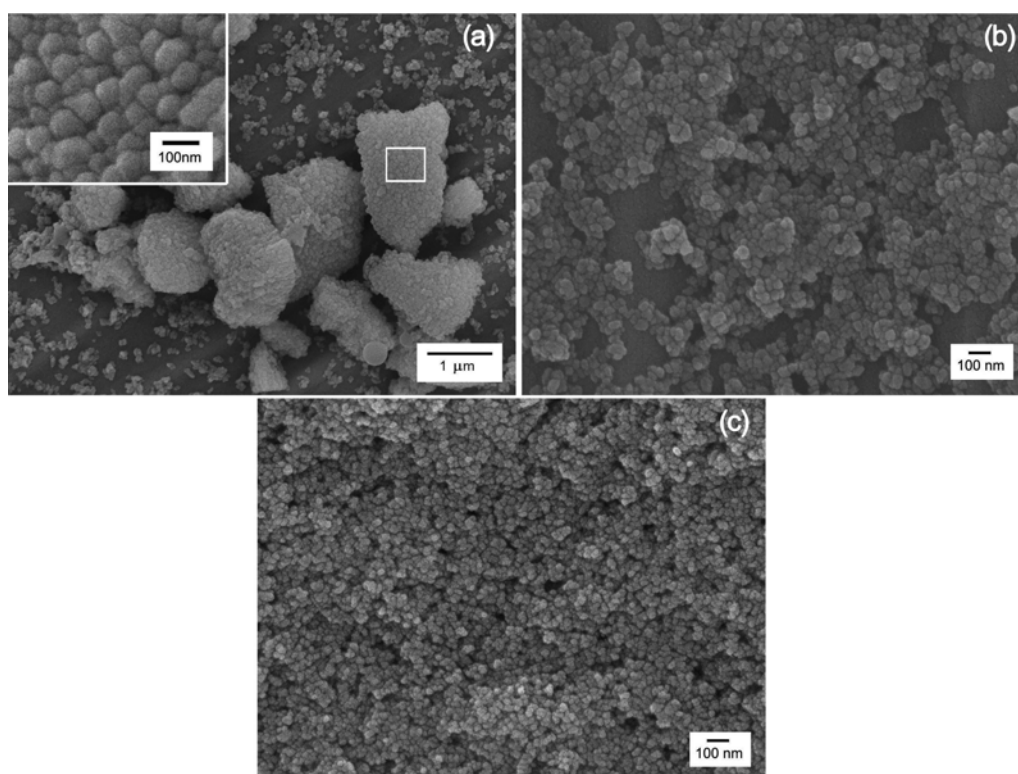


Fig. 3. SEM micrographs of the CaWO₄ powders prepared in different solvents: (a) pure water, (b) glycerol-water and (c) propylene glycol-water. (Insets are shown at higher magnification.)

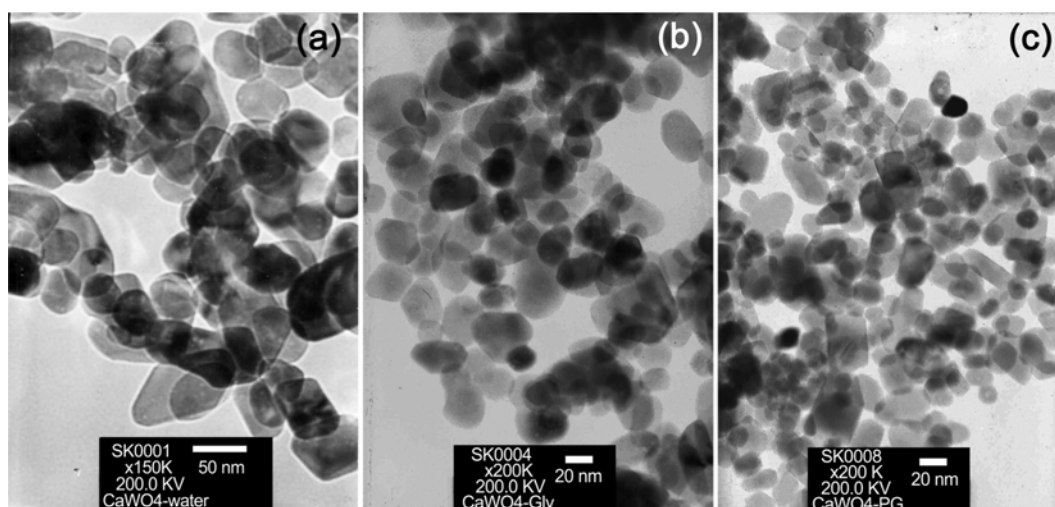


Fig. 4. TEM micrographs of CaWO₄ powders prepared in different solvents: (a) pure water, (b) glycerol-water and (c) propylene glycol-water.

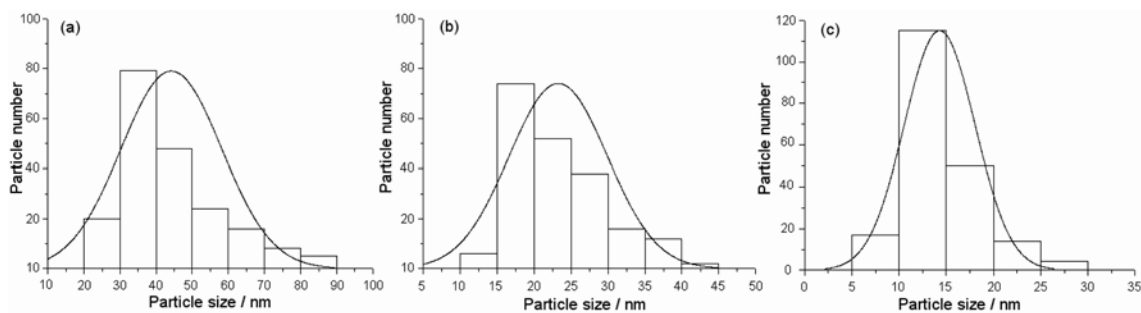


Fig. 5. Particle size distributions of CaWO₄ prepared in different solvents: (a) pure water, (b) glycerol-water and (c) propylene glycol-water.

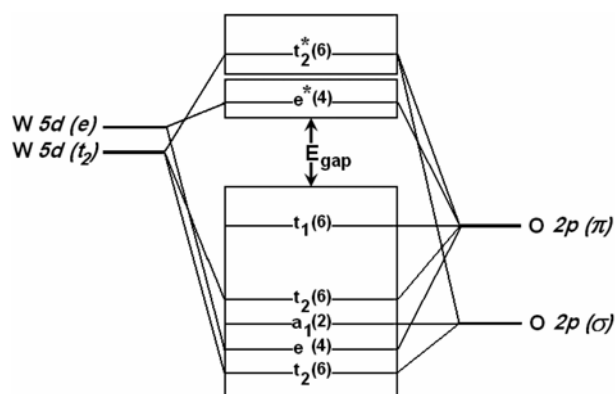
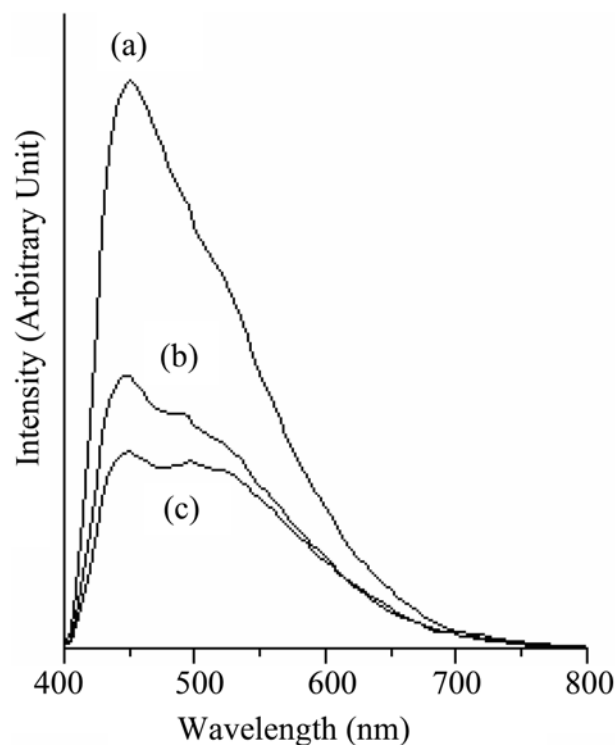
Table 1. Physical and chemical data of solvents utilized in the present research [16]

Solvent	Water	Glycerol	Propylene glycol
Molecular formula	H_2O	$\text{C}_3\text{H}_8\text{O}_3$	$\text{C}_3\text{H}_8\text{O}_2$
Molecular weight	18.02	92.09	76.10
Boiling point ($^{\circ}\text{C}$)	100	290	187.6
Density (g cm^{-3} , 20 $^{\circ}\text{C}$)	0.997	1.2613	1.0361
Dielectric constant (20 $^{\circ}\text{C}$)	80.1	46.53	27.5
Thermal conductivity (W/m K , 25 $^{\circ}\text{C}$)	0.607	0.292	0.200

size of CaWO_4 .

Metal tungstate crystallizes in the scheelite structure with tightly bound $(\text{WO}_4)^{2-}$ molecular ions loosely bound to M^{2+} cations. It is generally thought that in materials such as tungstate and molybdates the observed absorption and fluorescence spectra are associated with transitions within the molecular anion groups. The absorption transitions are attributed to charge transfer transitions in which an oxygen 2p electron goes into one of the empty tungsten 5d orbitals [20]. The crystal-field splitting and hybridization of the molecular orbitals of $(\text{WO}_4)^{2-}$ tetrahedra [22] are shown in Fig. 6. The $\text{W } 5d(t_2)$ and $\text{W } 5d(e)$ orbitals are hybridized with the $\text{O } 2p(\sigma)$ and $\text{O } 2p(\pi)$ ligand orbitals to form $(\text{WO}_4)^{2-}$ tetrahedra. The four ligand $p(\sigma)$ orbitals are compatible with the tetrahedral representation for a_1 and t_2 symmetries and the eight ligand $p(\pi)$ orbitals are for t_1 , t_2 and e symmetries. The top occupied state has t_1 symmetry formed from $\text{O } 2p(\pi)$ states. The lowest unoccupied state has e symmetry formed from a combination of the $\text{W } 5d(e)$ and $\text{O } 2p(\pi)$ orbitals to give antibonding (*). The hybridization between the $\text{W } 5d$ and $\text{O } 2p$ orbitals is specified as covalent bonding between the ions. For the ground state system, all one-electron states below the band gap are filled, resulting in a many-electron 1A_1 state. At the lowest excited state, there is one hole in the t_1 (primarily $\text{O } 2p(\pi)$) state and one electron in the e (primarily $\text{W } 5d$) state which give rise to many-electron 1T_1 , 3T_1 , 1T_2 and 3T_2 states. Among them, only the $^1T_2 \rightarrow ^1A_1$ transition is an electric dipole-allowed transition [20–22].

For the present research, the photoluminescent (PL) spectra of CaWO_4 have a similar shape due to the similarity in the morphologies. Fig. 7 shows the emission spectra of the CaWO_4 powders ($\lambda_{\text{ex}} = 283 \text{ nm}$). The PL emission at 444 nm wavelength is due to the $^1T_2 \rightarrow ^1A_1$ transition of electrons within $(\text{WO}_4)^{2-}$ anions [21–23]. The broad shoulders are from some defect centers with respect to oxygen, and interpreted as extrinsic transitions. The PL intensity for the powders prepared in pure water, which shows a large particle size, is the highest and controlled by the number of charge transfers. The strong luminescence intensity indicates the good crystallinity. It is obvious that PL intensities are decreased with a decrease of the particle sizes. These show that the solvents play a role in the product formations, morphologies, particle sizes and PL intensities. It is well known that the luminescent

**Fig. 6.** A schematic diagram of the crystal-field splitting and hybridization of the molecular orbitals of a tetrahedral WO_4^{2-} tetrahedron. E_{gap} indicates the energy band gap. “*” indicates antibonding (unoccupied) states. The boxes are included to emphasize the fact that the discrete states are broadened by neighboring cluster interactions in the solid material. The number in parentheses indicates the degeneracy of the $(\text{WO}_4)^{2-}$ complex.**Fig. 7.** PL spectra of CaWO_4 powders prepared in different solvents: (a) pure water, (b) glycerol-water and (c) propylene glycol-water.

properties of solids greatly depend on their particle size and morphology. This relationship is of current interest, and may lead to new fabrication processes to yield high quality luminescent materials.

Conclusions

CaWO_4 nanoparticles with different sizes were produced at 160 $^{\circ}\text{C}$ for 6 h by solvothermal reactions in different solvents. They provided the evidence of the scheelite

structure with W-O stretching vibration in $[\text{WO}_4]^{2-}$ tetrahedra at $705\text{--}875\text{ cm}^{-1}$. Photoluminescence (PL) emissions were detected at 444 nm due to the $^1\text{T}_2 \rightarrow ^1\text{A}_1$ transition of $(\text{WO}_4)^{2-}$ tetrahedra.

Acknowledgements

We are extremely grateful to the Thailand Research Fund (TRF), Commission on higher Education, National Research Council of Thailand (NRCT), and Naresuan University (Thailand) for financial support.

References

1. G. Zhou, M. Lu, B. Su, F. Gu, Z. Xiu and S. Wang, *Opt. Mater.*, 28 (2006) 1385-1388.
2. X. Zhang, Y. Xie, F. Xu and X. Tian, *J. Colloid Interf. Sci.*, 274 (2004) 118-121.
3. Z. Luo, H. Li, J. Xia, W. Zhu, J. Guo and B. Zhang, *J. Cryst. Growth*, 300 (2007) 523-529.
4. J.H. Ryu, J.W. Yoon and K.B. Shim, *Solid State Comm.*, 133 (2005) 657-661.
5. J.H. Ryu, C.S. Lim and K.H. Auh, *Mater. Lett.*, 57 (2003) 1550-1554.
6. Y. Wang, J. Ma, J. Tao, X. Zhu, J. Zhou, Z. Zhao, L. Xie and H. Tian, *Mater. Sci. Engin. B.*, 130[1-3] (2007) 277-281.
7. J.H. Ryu, J.W. Yoon, C.S. Lim, W.C. Oh and K.B. Shim, *Ceram. Inter.*, 31 (2005) 883-888.
8. Z. Lou and M. Cocivera, *Mater. Res. Bull.*, 37 (2002) 1573-1582.
9. V. Thangadurai, C. Knittlmayer and W. Weppner, *Mater. Sci. Engin. B*, 106 (2004) 228-233.
10. Powder Diffract. File, JCPDS Internat. Centre Diffract. Data, PA 19073-3273, U.S.A., 2001.
11. B. Smith, *Infrared Spectral Interpretations*, CRC Press, NY, (1999).
12. G.M. Clark and W.P. Doyle : *Spectrochim. Acta*, 22 (1966) 1441.
13. J.A. Gadsden : *Infrared Spectra of Minerals and Related Inorganic Compounds*, Butterworths, (1975).
14. D. Andreescu, E. Matijević and D.V. Goia, *Physicochemical and Engineering Aspects*, 291 (2006) 93-100.
15. R.M. Silverstein and F.X. Webster, "Spectrometric Identification of Organic Compounds", 6th Edition, John Wiley & Sons Inc, (1998) 88.
16. D.R. Lide and H.P.R. Fredrikse, "CRC Handbook of chemistry and physics", 76th Edition, CRC Press, Inc., New York, 1995-1996.
17. S. Yin, M. Shinozaki and T. Sato, *J. Lumin.*, 126 (2007) 427-433.
18. X.B. Zhao, X.H. Ji, Y.H. Zhang and B.H. Lu, *J. Alloys Comp.*, 368 (2004) 349-352.
19. Z. Hua, X.M. Wang, P. Xiao and J. Shi, *J. Eur. Ceram. Soc.* 26 (2006) 2257-2264
20. M.J. Treadaway and R.C. Powell, *J. Chem. Phys.* 61 (1974) 4003-4011.
21. Y. Zhang, N.A.W. Holzarwarth and R.T. Williams, *Phys. Rev. B*, 57 (1998) 12738-12750.
22. W.M. Yen, S. Shionoya and H. Yamamoto, "Phosphor Handbook," CRC Press/Taylor and Francis, (2006) 202.
23. V. B. Mikhailik, I. K. Bailiff, H. Kraus, P. A. Rodnyi and J. Ninkovic, *Radiat. Measur.*, 38 (2004) 585-588.